



## Characterization of signal kinetics in real time surgical tissue classification system

Markus Karjalainen<sup>a,b,\*</sup>, Anton Kontunen<sup>a,b</sup>, Anna Anttalainen<sup>b</sup>, Meri Mäkelä<sup>b</sup>, Soma Varga<sup>c</sup>, Maiju Lepomäki<sup>d,e</sup>, Osmo Anttalainen<sup>b</sup>, Pekka Kumpulainen<sup>b</sup>, Niku Oksala<sup>b,d,f</sup>, Antti Roine<sup>b</sup>, Antti Vehkaoja<sup>a</sup>

<sup>a</sup> Sensor Technology and Biomeasurements, Faculty of Medicine and Health Technology, Tampere University, Hervanta Campus, Korkeakoulunkatu 3, FI-33720 Tampere, Finland

<sup>b</sup> Olfactomics Ltd, Kampusareena, Korkeakoulunkatu 7, FI-33720 Tampere, Finland

<sup>c</sup> Pázmány Péter Catholic University, Faculty of Information Technology and Bionics, Budapest Práter u. 50/A 1083, Hungary

<sup>d</sup> Surgery, Faculty of Medicine and Health Technology, Tampere University, Kauppi Campus, Arvo Building, Arvo Ylpön katu 34, FI-33520 Tampere, Finland

<sup>e</sup> Department of Pathology, Fimlab Laboratories, Arvo Ylpön katu 4, FI-33520 Tampere, Finland

<sup>f</sup> Vascular Centre, Tampere University Hospital, Central Hospital, P.O. Box 2000, FI-33521 Tampere, Finland

### ARTICLE INFO

#### Keywords:

Differential ion mobility spectrometry  
Surgical margin analysis  
Tissue classification  
Signal carry-over

### ABSTRACT

Effective surgical margin assessment is paramount for good oncological outcomes and new methods are in active development. One emerging approach is the analysis of the chemical composition of surgical smoke from tissues. Surgical smoke is typically removed with a smoke evacuator to protect the operating room staff from its harmful effects to the respiratory system. Thus, analysis of the evacuated smoke without disturbing the operation is a feasible approach. Smoke transportation is subject to lags that affect system usability. We analyzed the smoke transportation delay and evaluated its effects to tissue classification with differential mobility spectrometry in a simulated setting using porcine tissues. With a typical smoke evacuator setting, the front of the surgical plume reaches the analysis system in 380 ms and the sensor within one second. For a typical surgical incision (duration 1.5 s), the measured signal reaches its maximum in 2.3 s and declines to under 10% of the maximum in 8.6 s from the start of the incision. Two-class tissue classification was tested with 2, 3, 5, and 11 s repetition rates resulting in no significant differences in classification accuracy, implicating that signal retention from previous samples is mitigated by the classification algorithm.

### 1. Introduction

Cancer is a major cause of death and disability. The majority of cancer patients are treated with surgery involving the excision of the tumor with clear margins to ensure that all of the tumor tissue is removed [1]. Margin assessment largely relies on palpation and visual examination by the surgeon in support with imaging (e.g., specimen radiography), frozen section analysis, and imprint cytology. These methods extend the operation time, only partially consider the resection margin, and may even lead to reoperation if the analysis is performed postoperatively. Less applied margin assessment methods include ultrasound imaging, optical methods, and radiofrequency spectroscopy. However, these disturb the normal surgical workflow and hence potentially delay the operation [2]. An ideal method should be accurate

and integrate into the existing devices and the surgical workflow.

Schäfer et al. proposed a method based on mass spectrometry (MS), in which the resected tissue is recognized from surgical smoke [3]. Analysis of surgical smoke is compelling since electrocautery is widely used in soft tissue surgery and an analyzer directly coupled with the surgical device could enable thorough margin assessment without disrupting the workflow. Another advantageous aspect is that the means to capture the smoke are already available, as smoke evacuation systems are widely used in operation rooms, and an analyzer could be coupled with these devices enabling contact-free margin assessment.

However, MS is a complex and resource-intensive technology. Our team has developed a differential mobility spectrometry (DMS) based system as a potential and more cost-effective alternative [4–6]. In order to enable the accurate localization and re-incision of the positive

\* Correspondence to: Tampere University, Korkeakoulunkatu 6, FI-33101 Tampere, Finland.

E-mail address: [markus.karjalainen@tuni.fi](mailto:markus.karjalainen@tuni.fi) (M. Karjalainen).

<https://doi.org/10.1016/j.snb.2022.131902>

Received 27 December 2021; Received in revised form 7 April 2022; Accepted 12 April 2022

Available online 22 April 2022

0925-4005/© 2022 The Author(s). Published by Elsevier B.V. This is an open access article under the CC BY license (<http://creativecommons.org/licenses/by/4.0/>).

margin, the surgeon requires rapid feedback. While the effect of delay has not been studied in this application, even relatively small latencies of 150–700 ms have been shown to affect the surgical performance in telesurgery [7–9]. Both MS and DMS-based systems are subject to delays caused by the limited sample gas flow rate, signal spreading due to flow profile, adhesion of molecules to the tubing as well as computing. Alongside latency, signal carry-over (i.e., the overlap between consecutive samples) is a significant challenge and likely the limiting factor for very fast systems.

The purpose of this study is to experimentally analyze the kinetics of an analytical system consisting of a standard smoke evacuator, sample pre-processing system, and DMS. The findings of this study provide a framework to all gas analysis systems that operate in time-sensitive applications.

## 2. Materials and methods

### 2.1. Experimental setup

Our experimental setup consists of commercial diathermy surgery equipment combined with a system intended for diathermy smoke analysis. The setup was constructed with the following devices: Itrakcut 350MB diathermy device (Innokas Medical, Finland); SafeAir® Smoke Evacuator compact surgical smoke evacuator (Stryker Corp, USA) with a 3-meter surgical evacuation tube and 50 l/min flow rate; Ionvision DMS spectrometer (Olfactomics Oy, Finland); and a custom-made filtration unit. We used commercial porcine muscle and renal tissues purchased from a local grocery store as the test sample.

We applied a nominal cutting power of 40 W and a frequency of 450 kHz to produce electrosurgical incisions to the porcine tissue samples. The surgical smoke produced by the incisions was analyzed by DMS. A DMS sensor device is essentially an electric field-tunable ion filter [9]. The filter has two separation electrode channels sized to  $6 \times 20 \times 0.25$  mm. Channel doubling enhances sensitivity by doubling the ion flow compared to a single channel. Electrodes are driven with two adjustable electrical field parameters, a high-frequency asymmetric alternating field, and a sequentially tuned constant compensation field. IonVision DMS can be flexibly set-up to sample the datapoints anywhere in its measurement range (any pair of high-frequency and compensation fields). Waveform generation is implemented as direct pulsing without resonators allowing for a rectangular pulse shape. The frequency of the separation field is adjustable from 250 kHz to 1 MHz. In this study, we used 1 MHz frequency. Separation field voltage is software-limited to 1 kV. Analog to digital converter (ADC) sampling rate is 333 kHz and features user-adjustable averaging between 1 and  $2^{15}$  samples. Used averages are presented in Table S1.

We used eleven pre-selected pairs of compensation and separation fields ranging from 0 to 22 V/mm and from 800 to 3668 V/mm, respectively. The field strengths and the number of averaged data points used in this study are provided in Table S1. Each DMS timepoint consisted of eleven datapoints from the positive and eleven datapoints from the negative ions. A small number of measurement points was used to enable high temporal sampling rate. We used forward feature selection from a detailed scan to select the used voltage pairs [10].

The filtration unit was an in-house developed prototype, of which the main purpose was to remove smoke particulates and deliver molecules to the spectrometer. The measurement setup is shown in Fig. 1. Transfer delays are estimated between the surgical scalpel, the filter and the spectrometer unit.

### 2.2. Description of variables

Time-dependent signals from the experiment setup were:

1. The diathermy current, which indicated the current flow through the porcine tissue

2. The corona discharge current in the filtration unit, in which the current was relative to the amount of smoke particulates and molecules
3. The DMS response to molecules. From these we derived six numerical indicators expressing the delay.

These times are illustrated in Fig. 1 and presented in Table 1.

### 2.3. Experiments

Two separate experiments were conducted to study the transfer line characteristics (the delays) and to assess the effect of delay on the performance of tissue classification. The experiments were executed with a fixed time delay to study transfer line kinetics and with a varying delay to assess its effect on classification. Data was captured with 3.7 Hz frequency in all experiments. The performance of tissue classification was evaluated using a shrinkage linear discriminant analysis (sLDA) model.

#### 2.3.1. Time series with fixed delays – kinetics testing dataset

The first dataset comprised tissue vapor impulses from 1.5 s electrocautery incisions to porcine renal cortex and skeletal muscle in a randomized order. Examples of data generated in this test are illustrated in Fig. 1. We repeated the incisions 50 times in 20 s intervals. Intervals were kept even so that all the remnants from the previous cut dissipated.

#### 2.3.2. Time series with varying delays – impulse interference effect for classifier

To study the effect of sampling (incision) intervals on the classification, we created a dataset in which the delays between the 1 s incisions varied between 2 s and 11 s (2, 3, 5, and 11 s). The one second incision duration was chosen to simulate a surgical procedure. Porcine renal cortex and skeletal muscle were incised in a randomized order. The dataset included ten subsets. Each of the first five subsets included twenty incisions, between which the order of the delays was the same for each repeat. The order of the tissues was the same for the first three and the next two sets.

For the latter five subsets, the order of the delays and tissues was randomized separately for each set. Also, the number of incisions was increased to 21 to fit 20 spaces in each set as illustrated in Fig. 2.

### 2.4. Data analysis

#### 2.4.1. Impulse response shape analysis

We studied the structure of signal tailing with curve fitting to understand the overall system behavior. An accurate tailing function would benefit the system simulations in later studies. Four different distribution functions were fitted to the averaged intensity responses obtained with the DMS data from 50 incisions. The distributions were inverse gaussian, Lévy distribution, lognormal distribution, and geometric Brownian motion distribution. Signals were synchronized by the time of a threshold crossing at the rising edge of a signal. For diathermy, we used a multiplier of 1.1 from the baseline level as the threshold level and for DMS, a multiplier of 1.6. The duration of the cuts varied around the targeted 1.5 s, which led to accumulation in the averaged peak shapes.

#### 2.4.2. Temporal classification

In the analysis of time dependency on tissue classification, we used leave-one-set-out as the cross-validation method. On each round, four sets were used as the training set and the fifth dataset was in turn assigned as the testing set. The datasets consisted of 50 randomized samples of porcine renal tissue and 50 randomized samples of porcine muscle. The intensity peaks were isolated to use individual time points for tissue classification. To remove linear drifting during the data collection, the data was detrended pixelwise based on the baseline values before each incision. For each time point in the extracted and

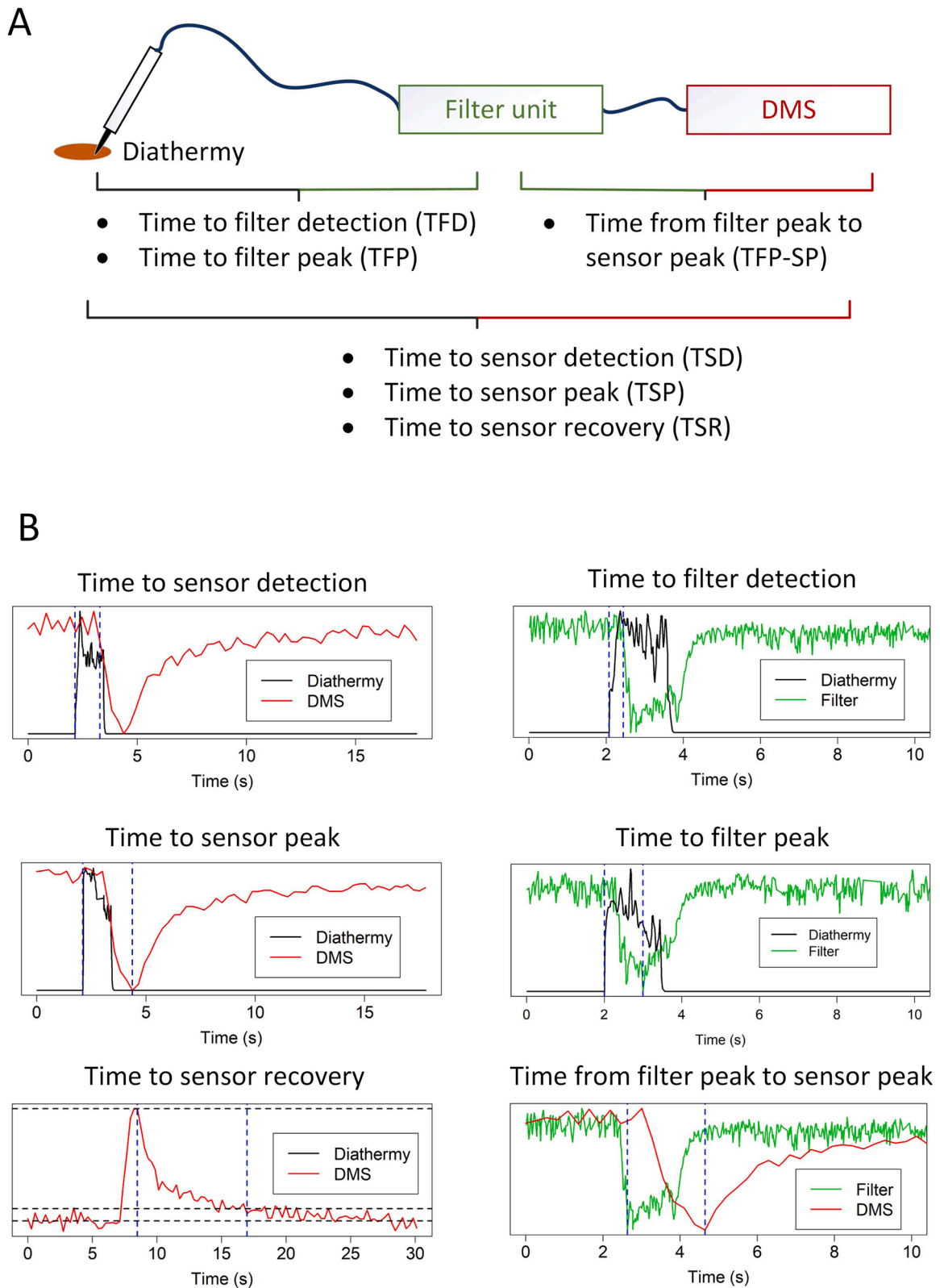


**Fig. 1.** Figurative explanations for the six delay indicators characteristic to each transfer line (A) and example signals visualizing the delays (B). Time to sensor detection describes the delay from the surgical incision to the first response in the DMS. Time to filter detection describes the time from the surgical incision to the filter unit. This is roughly the delay in the surgical tube. Time to sensor peak describes the delay from the incision to the peak response in DMS. Time to filter peak describes the delay from the incision to the strongest response in the filter unit. Time to sensor recovery describes the delay from the maximum signal to the 10% level of the baseline. Time from filter peak to sensor peak describes the delay in the device without the surgical tube.

**Table 1**  
Delay indicators used to characterize and quantify transport kinetics.

Indicator	Description
Time to sensor detection (TSD)	Delay from the beginning of the dissection to the beginning of the DMS response
Time to sensor peak (TSP)	Delay from the beginning of the dissection to the DMS signal maximum
Time to sensor recovery (TSR)	Decay time from the DMS signal maximum to the 10% level from the baseline
Time to filter detection (TFD)	Delay from the dissection beginning to the first response in the filter
Time to filter peak (TFP)	Delay from the dissection beginning to the maximum corona filter current
Time from filter peak to sensor peak (TFP-SP)	Delay between the corona filter maximum current and the DMS maximum signal

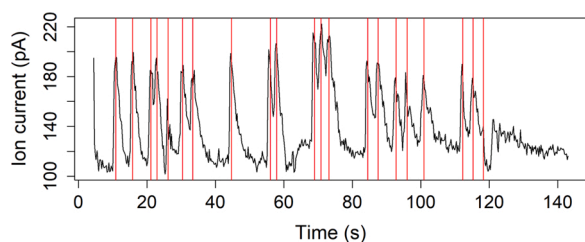


**Fig. 2.** One fifth of the randomized delay dataset from a single voltage pair channel. Red vertical lines indicate peaked signals, where classification is analyzed.

synchronized signals, separate, cross-validated (sLDA) classification models were created, and the classification accuracy was reported as a function of time from the peak signal strength. Impulse tailing interferes with later impulses. Therefore, we also studied how these earlier impulses affect the classification results. We studied how the classifier performs as a function of the time from the previous signal peak at the highest intensity value. In this analysis, the classifier was also trained with the leave-one-set-out method.

#### 2.4.3. Similarity metrics between tissue types

To evaluate the generalizability of animal tissue signal kinetics to actual surgery, we compared our data to measurements from a separate study with malignant and benign breast tissues [11]. These tissue samples were vaporized by a CO<sub>2</sub>-laser and analyzed with DMS. The samples included 192 measurements from two breast cancer specimens. We estimated the similarity between malignant and benign breast tissue, and between muscle and renal tissue by using the Euclidian distance of the classes from the respective archetypes (mean spectrums) of benign breast tissue and renal tissue. The Euclidean distance depicts the shortest distance between the two data vectors and can thus be used to estimate the relative differences of sample distributions [12]. If the relative differences between the tissue types are similar, we can expect similar temporal classification behavior.

### 3. Results

#### 3.1. Delay induced during sample transfer

After sample incision, the first response is measured from the diathermy current probe. Second, as the smoke reaches the filter unit, the current in the corona discharge changes. Last, the molecules reach the DMS sensor unit. The delayed signal is illustrated in Fig. 3.

The smoke evacuator tube used in the study was three meters long with a 10 mm inner diameter. Thus, the volumetric flow rate would approximate to 50 l/min and the travel time of an ideal plug flow to 300 ms. However, we recorded a mean delay of 340 (SD 170) ms. Similarly, an ideal plug flow from the corona discharge of the filter to

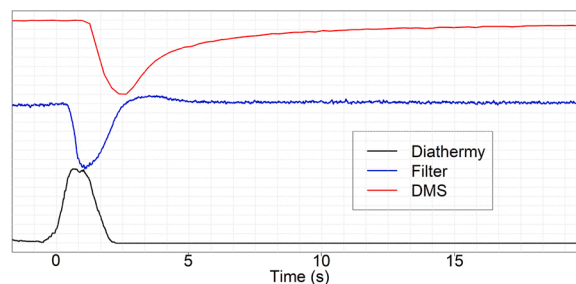


**Fig. 3.** Averaged and synchronized molecular transfer delays in the surgical sampling system.

DMS detection would be 350 ms. However, the recorded delay (TSD-TFD) was more than 700 ms.

The first detectable signal in the DMS was measured 1.1 (SD 0.3) seconds after the beginning of cutting. Then, the intensity increased for approximately 1.2 s and diminished to under 10% from the maximum within 8.2 (SD 2.3) seconds. All measured delays had outliers due to irregularities in the manual sampling. The delay distributions are presented as boxplots (Fig. 4).

We modeled the averaged impulse response with four heavy tailed distributions. The best fit was obtained with the Lévy distribution, a special case of inverse gaussian distribution, followed from a Lévy random walk [13]. The result is illustrated in Fig. 5. Other functions included the Log-normal, which is a maximum entropy probability distribution, and Geometric Brownian motion distribution, which follows the random walk with a gaussian distribution. The residual standard errors for the fittings were as follows: Lévy distribution 0.030, Inverse gaussian 0.037, Log-normal 0.047, and geometric Brownian motion 0.052, respectively. None of the fitting functions managed to describe the extra heavy tail after the peak well. The properties of the handmade input impulse affected the signal. The duration and the incision depth varied considerably and thus affected the sample concentration.

Based on the impulse response test, the classification accuracy of renal cortex and skeletal muscle correlated with the average signal intensity of the test set with some delay (Fig. 6). However, decaying of the signal weakened the classification. Many of the 11 voltage pair channels on higher separation field values posed lower signal-to-noise ratios than the channel illustrated in Fig. 6. Although an increase in the DMS separation field enhances ion cluster separation, it simultaneously decreases ion passing. As high electric field increases the movement amplitude of the ions it concurrently increases the probability of ion collisions to the separation electrodes, which neutralizes the ions. This phenomenon decreases the signal strength. It is noteworthy that there is similarly a high time-dependent noise in the classification accuracy.

#### 3.2. The effect of signal carry-over on the classification accuracy

The measurements concerning the effect of carry-over on the classification accuracy did not reveal a specific threshold time for unsuccessful classification. We utilized variable delay times and the classification was tested at peak intensities (Fig. 2). For 2, 3, 5, and 11 second intervals, there were no statistically significant differences. Both datasets consisted of 25 points per delay value. Classification accuracies are presented in Table 2. Herein, all ten partially and totally randomized subsets are combined. The results showed no observable trend as a function of delay time. It is worth noting that these delay times were instructed to the knife operator. Due to the manual operation, the actual delay times had some variance. These delay time distributions are presented in the supporting material Fig. S1. The distributions revealed few outliers caused by errors in the manual sampling. In addition, the correlation between the actualized delay times and the classification showed no clear bias (Fig. S2).

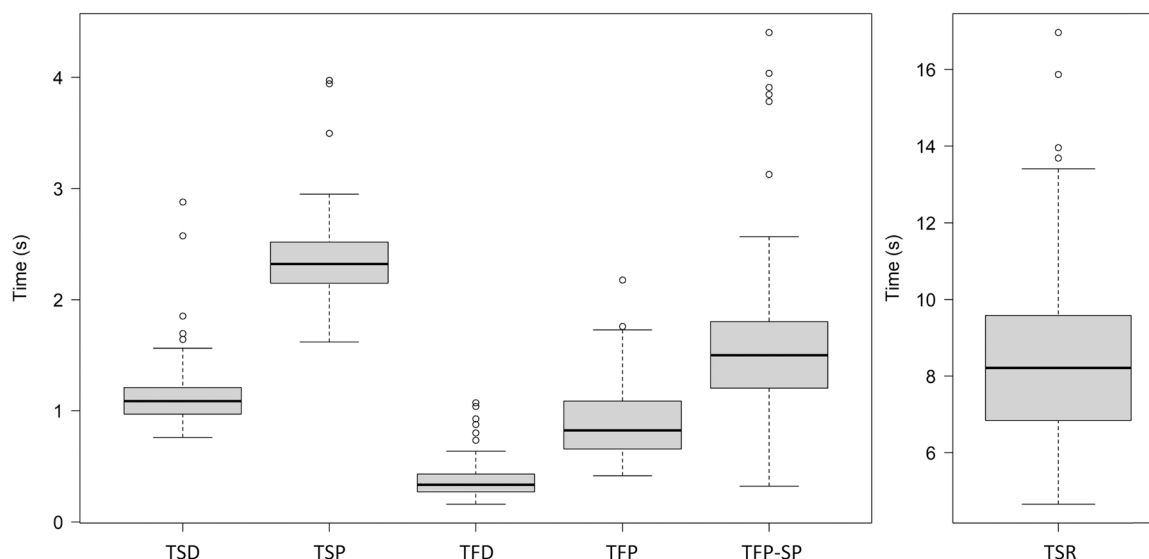


Fig. 4. Distributions of the delay indicator values are illustrated as boxplots. The dataset delay distributions are illustrated for each indicator parameter.

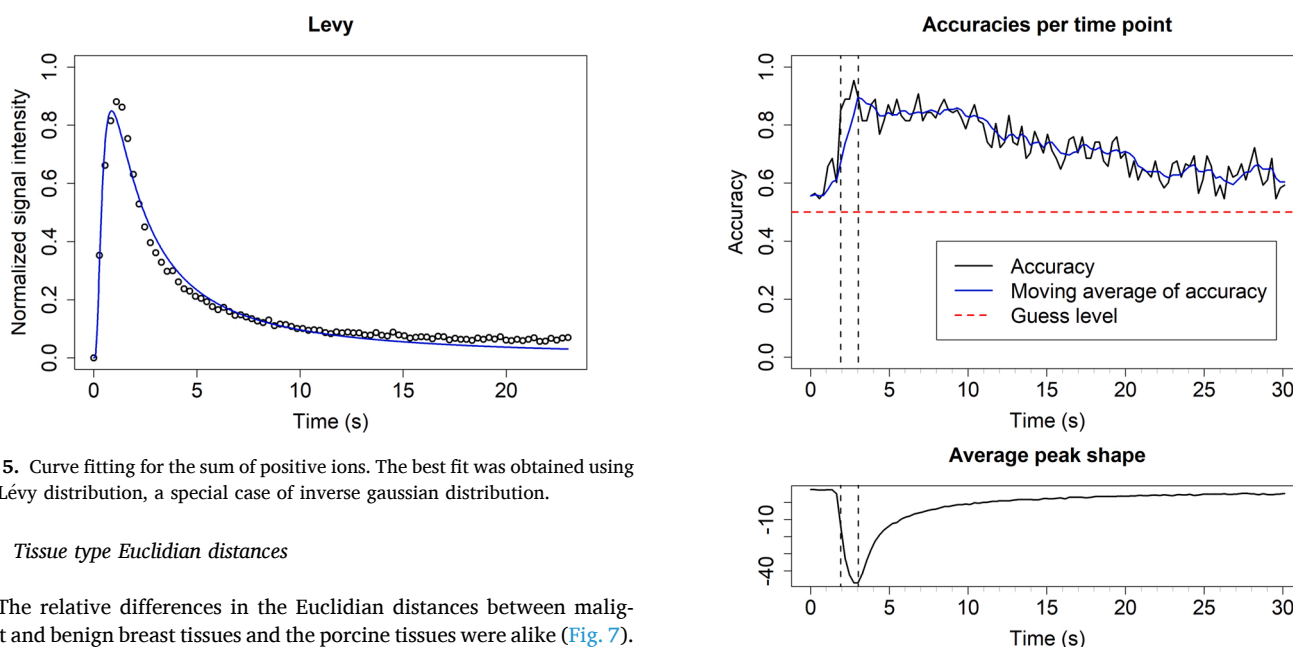


Fig. 5. Curve fitting for the sum of positive ions. The best fit was obtained using the Lévy distribution, a special case of inverse gaussian distribution.

### 3.3. Tissue type Euclidian distances

The relative differences in the Euclidian distances between malignant and benign breast tissues and the porcine tissues were alike (Fig. 7). Median Euclidian distance of individual malignant tissue samples to benign archetype was 0.59, and for benign tissue samples 0.44. The median Euclidian distance of individual muscle tissue samples to kidney archetype was 0.92, and individual kidney samples to kidney archetype 0.83. This finding suggests that the results of the study are also expected to be generalizable to clinically relevant tissues.

## 4. Discussion

In this study we shed light on the kinetics of gas detector systems for surgical tissue assessment with a well-controlled mechanistic model. The characteristics of the system are well comparable to those documented with mass spectrometers and further validate the potential of these technologies in surgical use.

Delay in the sample analysis greatly affects the usability and practical applicability of the device. We observed an average delay of 1.12 (SD 0.3) seconds from tissue contact to sensor detection. This is comparable to mass spectrometer-based systems, such as the iKnife system which has a delay from 0.7 to 2.5 s [14] or 1.8 (SD 0.40) seconds [15],

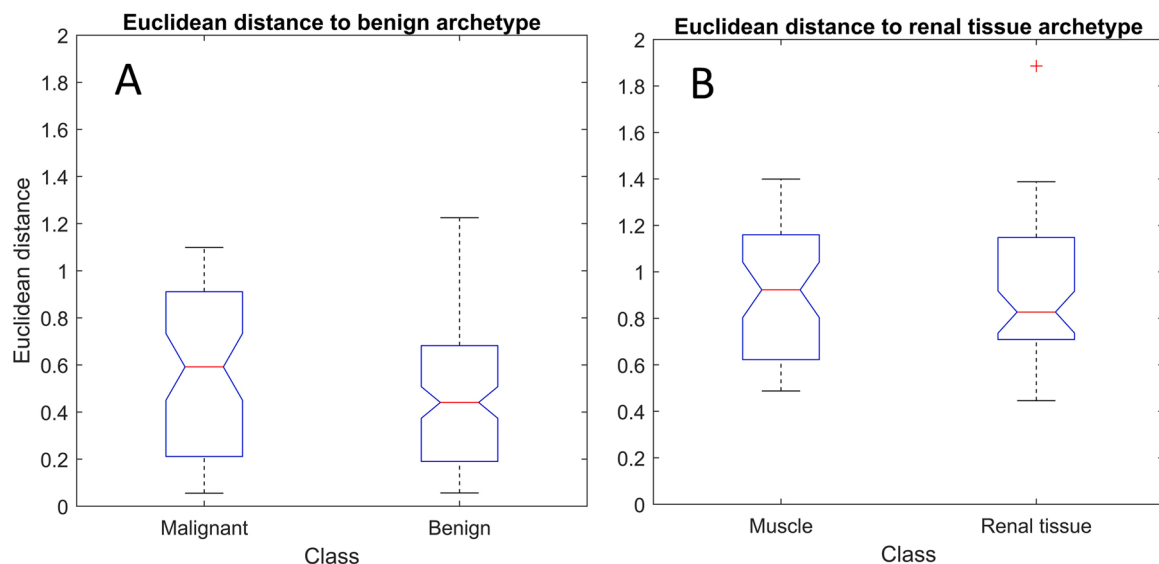
Fig. 6. The classification accuracy for impulse response. A decaying signal weakened the classification accuracy. After 7–8 s from the impulse peak, the classification accuracy decreased significantly. The average peak shape with the separation voltage (Usv) of 200 V and compensation voltage (Ucv) of 0.5 V.

Table 2

The classification accuracies alongside 95% confidence intervals for different delay times. Notably, there are no statistically significant differences in the accuracies.

Delay	Accuracy	95% confidence interval lower limit	95% confidence interval upper limit
1 s	0.74	0.56	0.85
2 s	0.80	0.66	0.90
4 s	0.82	0.69	0.91
10 s	0.71	0.56	0.84





**Fig. 7.** A) The distributions of the Euclidean distances between malignant and benign breast tissue compared to the benign archetype. B) The distributions of the Euclidean distances between muscle and renal tissue compared to the renal tissue archetype.

but is greater than delays documented for SpiderMass system ( $0.4 \text{ s} \pm 0.1$ ) [16]. In contrast to our system, which is an add-on to existing smoke evacuators, the iKnife and Spidermass utilize integrated tubing to enable the control of the tube diameter and flow rate. This evidently improves the time to detection. In this study, the TFD was less than half of the TSD implicating that the majority of the delay originated from the pneumatics of the prototype system. In addition to the smoke arrival delay, there is a data acquisition delay of around 200 ms and a data processing delay of around one second in our prototype system. However, these delays can be largely eliminated by increasing computing power and optimizing communication.

Even though the time to detection is rapid and sufficient for clinical use, the residual time of the molecules in the system is long at 8.6 s. This finding is in line with a previous MS study, where increase in the flow rate had a lesser effect on the retention time than on the time to detection [16]. Practical real-time use requires an ability to tolerate signal carry-over to an extent. We assessed this perspective by conducting electrocautery incisions in a random order with randomized delays on two different tissues. Surprisingly, we observed similar classification accuracies across the sampling intervals from 2 to 11 ss with a relatively simple sLDA model despite significant carry-over from the previous measurements. However, we hypothesize that the performance would decay at intervals below 2 s. The achieving of such sub-second intervals with a similar study setup would require computer-controlled sampling which may otherwise not be comparable to a human user. Additionally, impulse type sampling is likely easier to classify than a smooth transition from one tissue to another. The reality during surgery is between these two cases. In a study observing electrocautery activation patterns by consultants and specialists, Meeuwen et al. documented average activation times from 1.4 to 2.3 s [17], resembling more pulsed than continuous smoke production. This is in line with our observations of the system in operation theatre use [18].

As illustrated in Fig. 6, the best classification performance was obtained at the signal peak at 1.1 s after initial detection. This is theoretically the optimal time point for classification due to its high signal-to-noise ratio. Correct classification is therefore possible very shortly after detection, which is ideal for practical use. It is worth noting that the classification accuracy does not decrease along with the decaying signal strength. Rather, there seems to be a minimum requirement for signal strength. In contrary to our expectations, the classification accuracy did not improve with longer recovery delays between cuts. The absolute rate of correct classification remained modest especially for fully randomized

delay. This is likely due to the relatively small sample size that does not enable the classifier to reach its full potential. However, the sample size is sufficient to detect the practically meaningful rate of relative classification between delays.

We found no relevant studies related to the effect of surgical margin detection latency on the usability of a surgery assisting device. Literature on latency focuses on telesurgeries, in which the acceptable latency is less than one second [8]. Considering only the time to detection, a latency in this range can be reached whereas taking the retention time into account, we consider a 2–3 s latency realistic for pneumatic systems like DMS and MS. As surgeons typically cut tissues at a pace of 5–15 mm/second [19,20], this latency is acceptable for the intended purpose of alarming of a positive margin during cancer surgery.

The analysis of kinetics in this study was conducted exclusively with benign porcine tissues. In order to assess the generalizability to relevant cancerous tissues, we conducted a similarity analysis of data from cancerous tissues and of porcine tissues in this study. The finding that the difference between grossly malignant and benign tissue is larger than the difference between kidney and muscle tissue is intuitively surprising but is likely explained with heterogeneity of healthy tissue. Additionally, molecular profiling studies have demonstrated pancreatic characteristics that exceed the difference between organs. Nevertheless, the findings should be interpreted cautiously and confirmed with more extensive experiments with both benign and malignant human tissues. [21,22].

In order to build a theoretical model for kinetics of surgical smoke analysis systems, we studied the distributions of the signals. Farsad et al., 2013 [23] and Na-Rae et al., 2018 [24] studied chemical pulse transfer under forced flow in ambient air without tubes. Due to diffusion, the impulse response should follow inverse gaussian distribution in forced flow and Lévy distribution when there is no flow [25]. However, in our application and experiment setup, forced flow in a tube was used. These conditions introduced additional effects, namely turbulence and sorption-desorption events to tube walls, into the setting. In sorption-desorption interaction, molecules hit and stick to the tube walls, which delays and stretches the chemical signal. Therefore, we can assume that the signal tail lasts longer than commonly used heavy tailed distributions can estimate. We discovered that the Lévy distribution, which is characterized by a heavy tail, described our system the best, but still lacked heaviness in the tail. We did not try any function combinations to improve the fitting. Another explanation for curve mismatch could be the long nonideal input impulse. In addition to impulse

response, the tube material, size, and temperature affect the overall delay [26]. An accurate model would be beneficial for the simulation of the system behavior.

The sample size was limited, which limits the reliability of the results, since noise and other sporadic system variations may have affected the results. sLDA classifier boundaries are in a linear dimensional space so it can only respond linearly to nonlinear phenomena. Other methods, such as convolutional neural networks (CNNs), could provide different results in terms of the effect of delay on the classification accuracy but require larger data sets to operate sufficiently [6]. Therefore, they were not evaluated in the study. In addition, manual sampling has limitations in its accuracy and reliability. However, these accuracy related factors unlikely affected the main conclusions of this study.

The delay comparison between the filter current and the DMS is not straightforward. If a molecule hits the tube wall, it is delayed. In contrast, particulates stick to the wall permanently. Therefore, the particulate signal consists only of non-delayed particulates and the molecular signal is slower than the particulate signal. In other words, the particulate signal does not have a heavy tail. In addition, particulates attached to the tube walls emit molecules. These factors enhance the difference between the filter and the DMS response. The filter responds to both molecules and particulates whereas the DMS responds only to molecules. In addition, in the filter, particulates decrease current caused by ion mobility, and molecules increase the mobility. This causes the two-directional response seen in Fig. 3 filter current.

## 5. Conclusions

The studied surgical smoke detection system has low latency on signal detection but suffers from long retention times. Surprisingly, the retention time does not have a significant effect on the correct classification rate. The sample impulses produce heavy tailed responses, which are best described by the Lévy distribution, although still lacking heaviness in tailing. The delays exhibited by the smoke analysis system are comparable to MS-based methods and are short enough to enable the surgical application of tissue identification based on surgical smoke. However, to maximize the applicability of the surgical smoke detection systems, a thorough optimization of tubing lengths, flow control, and computational integration are required.

## CRedit authorship contribution statement

**Markus Karjalainen:** Conceptualization, Investigation, Writing – original draft. **Anton Kontunen:** Investigation, Validation, Formal analysis, Writing – review & editing. **Anna Anttalainen:** Software, Validation, Data curation, Visualization, Writing – review & editing. **Meri Mäkelä:** Investigation, Data curation, Writing – review & editing. **Varga Soma:** Investigation, Validation, Writing – review & editing. **Maiju Lepomäki:** Investigation, Formal analysis – review & editing. **Osmo Anttalainen:** Resources, Writing – review & editing. **Pekka Kumpulainen:** Validation, Investigation, Writing – review & editing. **Niku Oksala:** Resources, Supervision, Funding acquisition, Review & editing. **Antti Roine:** Conceptualization, Supervision, Writing – original draft and Review & editing. **Antti Vehkaoja:** Supervision, Project administration, Writing – review & editing.

## Declaration of Competing Interest

The authors declare the following financial interests/personal relationships which may be considered as potential competing interests: Markus Karjalainen reports a relationship with Olfactomics Ltd. that includes: employment and equity or stocks. Anton Kontunen reports a relationship with Olfactomics Ltd. that includes: employment and equity or stocks. Anna Anttalainen reports a relationship with Olfactomics Ltd. that includes: employment. Meri Makela reports a relationship with Olfactomics Ltd. that includes: employment. Osmo Anttalainen reports a

relationship with Olfactomics Ltd. that includes: employment and equity or stocks. Pekka Kumpulainen reports a relationship with Olfactomics Ltd. that includes: employment and equity or stocks. Niku Oksala reports a relationship with Olfactomics Ltd. that includes: equity or stocks. Antti Roine reports a relationship with Olfactomics Ltd. that includes: employment and equity or stocks.

## Acknowledgements

Markus Karjalainen declares funding from The Finnish Cultural Foundation, Pirkanmaa Regional Fund, Finland. Anton Kontunen declares funding from the Doctoral School of the Faculty of Medicine and Health Technology, Tampere University, and Emil Aaltonen Foundation, Finland (Grant number 210073). Maiju Lepomäki declares funding from the Doctoral School of Tampere University, the Finnish Medical Foundation (Grant numbers 2167, 4038), and Cancer Foundation of Finland. Niku Oksala declares funding from Competitive State Research Financing of the Expert Responsibility area of Tampere University Hospital, Finland (Grant numbers 9s045, 9T044, 9U042, 150618, 9V044, 9 × 040, 9AA057, 9AB052 and MK301); from Competitive funding to strengthen university research profiles funded by Academy of Finland, Finland, decision number 292477; and from Tampereen Tuberkuloosisäätiö (Tampere Tuberculosis Foundation). Olfactomics has received funding from the European Union's Horizon 2020 research and innovation programme, EU under grant agreements No 848682.

The study sponsors did not have any involvement in the study design; collection, analysis, and interpretation of data; the writing of the manuscript; or the decision to submit the manuscript for publication.

## Appendix A. Supporting information

Supplementary data associated with this article can be found in the online version at [doi:10.1016/j.snb.2022.131902](https://doi.org/10.1016/j.snb.2022.131902).

## References

- [1] B.W. Maloney, D.M. McClatchy III, B.W. Pogue, K.D. Paulsen, W.A. Wells, R. J. Barth, Review of methods for intraoperative margin detection for breast conserving surgery, *J. Biomed. Opt.* 23 (10) (2018), 100901.
- [2] J. Schwarz, H. Schmidt, Technology for intraoperative margin assessment in breast cancer, *Ann. Surg. Oncol.* 27 (2020) 2278–2287.
- [3] K.-C. Schäfer, et al., In vivo, in situ tissue analysis using rapid evaporative ionization mass spectrometry, *Angew. Chem. Int. Ed.* 48 (44) (2009) 8240–8242.
- [4] M. Sutinen, et al., Identification of breast tumors from diathermy smoke by differential ion mobility spectrometry, *Eur. J. Surg. Oncol.* 45 (2) (2019) 141–146.
- [5] I. Haapala et al., "Identifying brain tumors and healthy brain tissue by direct ion mobility spectrometry analysis of diathermy smoke," 2017.
- [6] A. Kontunen, et al., Real time tissue identification from diathermy smoke by differential mobility spectrometry, *IEEE Sens. J.* 21 (1) (2020) 717–724.
- [7] A. Kumcu, et al., Effect of video lag on laparoscopic surgery: correlation between performance and usability at low latencies, *Int. J. Med. Robot. Comput. Assist. Surg.* vol. 13 (2) (2017), e1758.
- [8] F. Richter, Y. Zhang, Y. Zhi, R.K. Orosco, and M.C. Yip, "Augmented reality predictive displays to help mitigate the effects of delayed telesurgery," in 2019 International Conference on Robotics and Automation (ICRA), 2019, pp. 444–450.
- [9] M.D. Fabrizio, et al., Effect of time delay on surgical performance during telesurgical manipulation, *J. Endourol.* 14 (2) (2000) 133–138.
- [10] M. Sutinen et al., "Identifying breast tumors and healthy breast tissue by differential ion mobility (DMS) spectrometry analysis of diathermy smoke (Talk)," 2017, [Online]. Available: [http://cofa.uta.fi/admin\\_cofa/wp-content/uploads/2017/04/BMT-MED-Research-Day-2017\\_Abstracts3.pdf](http://cofa.uta.fi/admin_cofa/wp-content/uploads/2017/04/BMT-MED-Research-Day-2017_Abstracts3.pdf).
- [11] L. Maiju, et al., Laser desorption tissue imaging with Differential Mobility Spectrometry, *Exp. Mol. Pathol.* (2022), 104759.
- [12] J. Virtanen, et al., Differentiation of aspirated nasal air from room air using analysis with a differential mobility spectrometry-based electronic nose: a proof-of-concept study, *J. Breath. Res.* 16 (2021).
- [13] A.V. Chechkin, R. Metzler, J. Klafter, V.Y. Gonchar, Introduction to the theory of Lévy flights (and others), *Anomalous Transp.* 129 (2008).
- [14] J. Balog, et al., "Intraoperative Tissue Identif. Using Rapid Evaporative Ioniz. Mass Spectrom.," vol. 5 (194) (2013) 194ra93, doi: 10.1126/SCITRANSLMED.3005623.
- [15] E.R. John St, et al., "Rapid evaporative ionisation mass spectrometry of electrosurgical vapours for the identification of breast pathology: towards an intelligent knife for breast cancer surgery, *Breast Cancer Res.* 19 (1) (2017) 1–14.
- [16] B. Fatou, et al., In vivo real-time mass spectrometry for guided surgery application, *Sci. Rep.* 6 (1) (2016) 1–14.

- [17] F.C. Meeuwse, A.C.P. Guédon, E.A. Arkenbout, M. van der Elst, J. Dankelman, J. J. Van Den Dobbelsteen, The art of electrosurgery: trainees and experts, *Surg. Innov.* 24 (4) (2017) 373–378.
- [18] A. Kontunen, et al., Tissue identification from surgical smoke by differential mobility spectrometry: an in vivo study, *IEEE Access* (1) (2021) doi: 10.1109/ACCESS.2021.3136719.
- [19] J. Liboon, W. Funkhouser, D.J. Terris, A comparison of mucosal incisions made by scalpel, CO<sub>2</sub> laser, electrocautery, and constant-voltage electrocautery, *Otolaryngol. Neck Surg.* 116 (3) (1997) 379–385.
- [20] S.T. Vedbhushan, M.A. Mulla, D.M. Chandrashekhar, Surgical incision by high frequency cautery (and others), *Indian J. Surg.* 75 (6) (2013) 440–443.
- [21] K.A. Hoadley, et al., Cell-of-origin patterns dominate the molecular classification of 10,000 tumors from 33 types of cancer, *Cell* 173 (2) (2018) 291–304.
- [22] E. Reznik, et al., A landscape of metabolic variation across tumor types, *Cell Syst.* 6 (3) (2018) 301–313.
- [23] N. Farsad, W. Guo, A.W. Eckford, Tabletop molecular communication: Text messages through chemical signals, *PLoS One* 8 (12) (2013), e82935.
- [24] N.-R. Kim, N. Farsad, C. Lee, A.W. Eckford, C.-B. Chae, An experimentally validated channel model for molecular communication systems, *IEEE Access* 7 (2019) 81849–81858.
- [25] Y. Murin, N. Farsad, M. Chowdhury, and A. Goldsmith, “Communication over diffusion-based molecular timing channels,” in 2016 IEEE Global Communications Conference (GLOBECOM), 2016, pp. 1–6.
- [26] M. Karjalainen, et al., Recovery characteristics of different tube materials in relation to combustion products, *Int. J. Ion.-. Mobil. Spectrom.* (2020) 1–8.

**Markus Karjalainen** received the M.Sc. degree in automation engineering from the Tampere university of Technology, Finland, in 2007. He is currently pursuing the D.Sc. degree with the Faculty of Medicine and Health Technology, Tampere University, Finland. From 2006–2017, he was with the Department of Automation Science and Engineering, Tampere University of Technology. He also works as a Hardware Engineer in a university spin-off company, Olfactomics Oy, Tampere, Finland. His research interests include chemical communication and sensor technology.

**Anton Kontunen** received the B.Sc. and M.Sc. degrees in bioengineering from the Tampere University of Technology, Finland, in 2015 and 2017, respectively. He received the D. Sc. degree from the Faculty of Medicine and Health Technology, Tampere University in 2022. From 2014–2017, he was a Research Assistant with the Department of Automation Science and Engineering, Tampere University of Technology. He also works as a System Engineer in a university spin off company, Olfactomics Oy, Tampere, Finland. His research interests include biomedical engineering, sensor technology, and data science.

**Anna Anttalainen** received the B.Sc. degree in bioinformation technology (major in computational and cognitive biosciences) and the M.Sc. degree in life science technologies (major in complex systems) from Aalto University, Finland, in 2016 and 2019, respectively. From 2014–2016, she was a Research Assistant with the Department of Neuroscience and Biomedical Engineering. From 2016–2019, she was an Assistant Teacher for a mathematical modeling course with Aalto University. She is currently pursuing a career in data science in Medafcon Oy, Espoo, Finland. Her research interests include machine learning with a focus on neural networks.

**Meri Mäkelä** received the M.Sc. degree in bioengineering (major in bio measurements and bioimaging) from Tampere University in 2020. She also works as a usability engineer in a university spin-off company, Olfactomics Oy, Tampere, Finland.

**Soma Varga** received B.Sc. degree in biochemical engineering and M.Sc. degree in Biotechnology from the Budapest University of Technology and Economics, Hungary, in 2019 and 2021, respectively. He is currently pursuing the Ph.D. degree in Pázmány Péter Catholic University, Faculty of Information Technology and Bionics. He was an exchange student as Biomedical Engineer in Tampere University, Finland in 2021. His research interests include spectroscopy, bioinformatics and biotechnology.

**Maiju Lepomäki** received the M.D. degree from Tampere University in 2018. She is currently pursuing the Ph.D. degree in medicine with the Faculty of Medicine and Health Technology, Tampere University. Since 2020, she has worked as a specializing physician at Fimlab Laboratories in the Department of Pathology. Her research interests are breast pathology, surgical oncology, and novel technologies in surgical margin assessment

**Osmo Anttalainen** received the M.Sc. degree in energy technology from the Lappeenranta University of Technology, Finland, in 1992. From 1994–2018, he was with Enviroics Oy, Mikkeli, Finland. He is currently continuing his career in a university spin-off company, Olfactomics Oy, Tampere, Finland. His research interests include ion mobility spectrometry and mixed signal electronics.

**Pekka Kumpulainen** received the M.Sc. and the D.Sc. (Tech.) degrees from the Tampere University of Technology in 1994 and 2014, respectively. From 1992–2019, he was with the Department of Automation Science and Engineering, Tampere University of Technology. Since 2019 he has been working as an independent consultant in data analytics.

**Niku Oksala** received the M.D. and Ph.D. degrees in medicine and experimental surgery from the University of Eastern Finland in 2000 and 2003, respectively, and the D.Sc. (Med.) degree in molecular biology from Tampere University, Finland, in 2009. Since 2007, he has been a Consultant Vascular Surgeon and a Clinical Teacher. Since 2014, He is currently a Professor of Vascular Surgery with the Faculty of Medicine and Health Technology, Tampere University, and also a Chief Vascular Surgeon with Tampere University Hospital. He has authored more than 200 international journal articles. His current research interests include biomedical sensor technology, clinical research, and molecular biology. He serves as a Board Member for the Instrumentarium Science Foundation and The Finnish Cardiovascular Research Center, Tampere, Finland. He is the Chairman of the Board and a CMO of Olfactomics Oy, Tampere, Finland.

**Antti Roine** received the M.D. degree from Tampere University, Finland, in 2014, and the Ph.D. degree from Tampere University, Finland, in 2014. Since 2014, he has been holding various positions as a Physician in surgery, emergency medicine, and family medicine. In this period, he has also acted as a Project Manager in healthcare digitalization in Tampere. He currently acts as the CEO of Olfactomics Oy. He is also an Active Researcher with Tampere University. His research interests include surgical oncology, gas sensors, and the application of artificial intelligence in medical applications.

**Antti Vehkaoja** received the M.Sc. degree in electrical engineering from the Tampere University of Technology, Finland, in 2004, and the D.Sc. (Tech.) degree in automation science and engineering from the Tampere University of Technology in 2015. He is currently an Associate Professor of Sensor Technology and Biomeasurements with the Faculty of Medicine and Health Technology, Tampere University. He has authored more than 100 international scientific articles. His research interests include sensors and embedded systems for biomedical applications and related signal processing and data analysis methods.